The Synthesis, Characterization, and DC Electrical Conductivity of Poly[di(2,5-dimercapto-1,3,4-thiadiazole)-Metal] Complexes

Ali G. El-Shekeil, Hussein M. Al-Maydama, Omar M. Al-Shuja'a

Department of Chemistry, Faculty of Science, Sana'a University, Sana'a, Yemen

Received 23 March 2006; accepted 6 April 2007
DOI 10.1002/app.26824
Published online 26 July 2007 in Wiley InterScience (www.interscience.wiley.com).

ABSTRACT: Poly[di(2,5-dimercapto-1,3,4-thiadiazole)]-metal complexes of Co(II), Ni(II), Cu(II), and Zn(II) were synthesized by the reaction of 2,5-dimercapto-1,3,4-thiadiazole (6.6 mmol) with anhydrous cobalt, nickel, copper, and zinc chlorides (3.3 mmol) in absolute ethanol under reflux for 24 h. The products were characterized by elemental analyses, electronic spectra, FTIR spectroscopy, as well as thermal analyses (TGA and DTA), and X-ray diffraction. The DC electrical conductivity variation of the poly[di(2,5-dimercapto-1,3,4-thiadiazole)-metal] complexes were studied in the temperature range 300–500 K as annealed for 24 h at 100°C and after doping with 5% I_2 for comparison. An attempt is made to interpret the DC electrical conductivity behavior and thermal properties to doping, annealing, structure, and metal used. © 2007 Wiley Periodicals, Inc. J Appl Polym Sci 106: 2427–2435, 2007

Key words: poly[di(2,5-dimercapto-1,3,4-thiadiazole)-metal] complexes; 2,5-dimercapto-1,3,4-thiadiazole; DC electrical conductivity; doping; thermal analysis; X-ray diffraction; activation energies

INTRODUCTION

2,5-Dimercapto-1,3,4-thiadiazole (DMT) and poly-DMT (PDMT) are interesting compounds that attracted the attention of researchers because of their wide applications in many fields such as, determination of trace elements, synthesis of novel heterocyclic compounds with antimicrobial activity,[1,2] advanced technology materials, and battery cathode.[3,4] Furthermore, the successful commercial applications of electrically conducting polymers have attracted the attention of researchers long time ago and triggered intensive research.[5–7] In addition to that, much attention has been directed to polymeric metal complexes by researchers with many contributions in applications such as, protective coatings, catalysts, semiconductors, and analytical methods.[8–10]

A new series of transition metal polymer complexes from PDMT and the chlorides of Co(II), Ni(II), Cu(II), and Zn(II) in the backbone of the chain was synthesized, characterized, and described in this study. The presence of four different 3D transition metals allowed the comparison of the chemical and physical properties: FTIR, UV-vis, thermogravimetric analyses (TGA), differential thermal analyses (DTA), and DC electrical conductivity. The most important part of this work is the comparative study of the DC electrical conductivity. Two states of DC electrical conductivity were studied: the annealed and 5% I_2 doped states with temperature variation in the range 300–500 K. The activation energies (E_a) are calculated from the DC electrical conductivity and thermal analyses.

Correspondence to: A. G. El-Shekeil (shekeil@yemen.net.ye).

Contract grant sponsor: TWAS; contract grant number: 02-011 LDC/CHE/AF/AC.

EXPERIMENTAL

Chemicals

The chemicals, synthesized or purchased (Aldrich chemicals), were recrystallized twice before use. The solvents were reagent grade: 99% absolute ethanol, dimethylformamide (DMF) (BDH, AnalaR®).

Synthesis of the polymer-metal complexes

A solution of the anhydrous metal chlorides of (Co(II), Ni(II), Cu(II), and Zn(II)) (3.3 mmol) in ethanol (25 mL) was added to a solution of 2,5-dimercapto-1,3,4-thiadiazole (6.6 mmol, 2.0 g) in the same solvent (25 mL). The mixture was refluxed with stirring for 24 h under a thin stream of nitrogen gas. The precipitated polymer was separated by filtration, then washed several times with hot ethanol and dried in the air for 24 h.

Instrumentation

The melting points were measured on an electrothermal melting point apparatus. FTIR spectra were

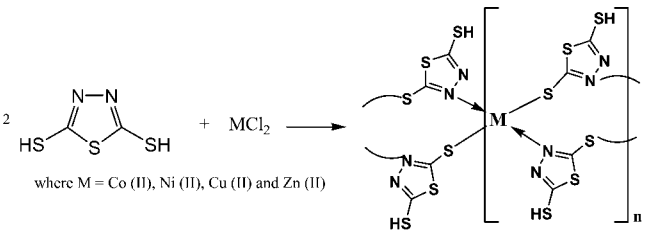

Scheme 1 The synthesis of the poly[di(2,5-dimercapto-1,3,4-thiadiazole)-metal complexes. (M = Co(II), Ni(II), Cu(II), and Zn (II).

recorded using the KBr disc technique on a Shimadzu 8101 FTIR Spectrophotometer. The elemental (CHNS) analyses were performed on an Elementar Analyses system GmbH Varioel $V_{2.3}$ 1998 CHNS Mode. The UV and visible absorption spectra were measured in DMF using a PU 8800 UV-visible spectrophotometer-Philips Automatic Scanning Spectrophotometer. Thermal analyses were conducted on a Shimadzu TGA-50H and Shimadzu DTA-50 at 25–1000°C under 20 mL nitrogen per minute and a heating rate of 10°C min^{-1}. X-ray diffraction was conducted on a Bruker Axs Da Advance diffractometer. The electrical conductivity measurements was measured on a Keithley Picoammeter/Voltage Source Model 6487. Doping and annealing were performed as described previously.[11]

Thermal analyses of the poly[di(2,5-dimercapto-1,3,4-thiadiazole)-metal] complex

The thermal decomposition behavior of the poly[di(2,5-dimercapto-1,3,4-thiadiazole)]-metal complexes was investigated by TGA and DTG. The thermograms (TG, DTG, and DTA curves) were obtained by using a Shimadzu thermogravimetric analyzer, TGA-50, at a heating rate of 20°C min^{-1} under 20 mL min^{-1} nitrogen flow and a heating program 23–1000°C.

For each step in the decomposition sequence, the following parameters were determined:

From DTG curves of decomposition, T_i was taken as the point at which the DTG curve begins to deviate from its base line as initial reaction and the point at which the DTG curve returns to its base line, was taken as a final temperature of decomposition T_f. The temperature of maximum rate of weight loss T_{DTG} is obtained from the intersection of tangents to the DTG peak.

From the TG curves, the weight loss at the decomposition step Δm is determined from the point T_i, the initial temperature of decomposition, up to the end of the reaction at the point T_f.

The activation energy E_a was calculated from the slope of a plot of the Coats-Redfern equation[12] for the reaction order $n \neq 1$. The order of reaction n is determined by the Horovitz-Metzger method[13]:

$$\mathrm{Ln}\left[\frac{1-(1-\alpha)^{1-n}}{T^2(1-n)}\right] = \mathrm{Ln}\frac{ZR}{qE}\left[1-\frac{2RT}{E}\right] - \frac{E}{RT}$$

where, α = fraction of weight loss, T = temperature (K), n = order of reaction, Z = pre-exponential factor, R = molar gas constant, E_a = activation energy, and q = heating rate.

RESULTS AND DISCUSSION

Synthesis and characterization

The poly[di(2,5-dimercapto-1,3,4-thiadiazole)]-metal complexes (Scheme 1) were prepared by the reaction of 2,5-dimercapto-1,3,4-thiadiazole (2 mol) with anhydrous cobalt, nickel, copper, and zinc chlorides (1 mol) in absolute ethanol under reflux for 24 h under a thin stream of nitrogen gas. Table I summarizes the physical properties (color, % yield, and CHNS) of the four polymer metal complexes.

All the materials showed melting points above 300°C. The reaction yields ranged from 30 to 63%. The color of the polymer complexes increased from white for zinc, dark yellow for copper to dark brown for nickel, and green in the case of cobalt.

The FTIR spectra

The main FTIR bands of the poly[di(2,5-dimercapto-1,3,4-thiadiazole)-metal] complexes are summarized in Table II. The assigned absorption bands are consistent with the suggested structures.

The stretch ν(S—H) weak band showed up weakly at (2491 cm^{-1}) and the deformation antisymmetric (δ_{as}) (C—SH) in-plane (ip) and deformation symmetric (δ_s) $(C—SH)_{ip}$ were also weak bands at (948 cm^{-1}, 923 cm^{-1}) respectively,[14] whereas all these bands showed up as very weak bands in the prod-

TABLE I
Characterization Data of Poly[di(2,5-dimercapto-1,3,4-thiadiazole-metal] Polymers Complexes

Polymer-metal complexes	Formula (mol. wt.)	Color (yield %)	CHNS % calcd. (found)			
			C	H	N	S
PDMT-Co	$C_4H_2CoN_4S_6$ (357.41)	Green (38)	13.44 (13.52)	0.56 (0.59)	15.68 (15.47)	53.83 (53.97)
PDMT-Ni	$C_4H_2N_4S_6Ni.6H_2O$ (465.26)	Dark-brown (30)	10.33 (9.96)	3.03 (3.08)	12.04 (12.35)	41.35 (41.16)
PDMT-Cu	$C_4H_2N_4S_6Cu.2H_2O$ (398.05)	Dark-yellow (63)	12.13 (11.86)	1.02 (0.85)	14.15 (14.54)	48.58 (48.38)
PDMT-Zn	$C_4H_2N_4S_6Zn$ (363.87)	White (33)	13.20 (13.25)	0.55 (0.45)	15.40 (15.27)	52.87 (53.18)

TABLE II
Main FTIR Bands of the Poly[di(2,5-dimercapto-1,3,4-thiadiazole)-metal] Complexes

Polymer-metal complexes	DMT	PDMT-Co	PDMT-Ni.6H_2O	PDMT-Cu.2H_2O	PDMT-Zn
ν (S—H)	2491 w	2491 vvw	2491 vvw	2491 vvw	2491 vvw
ν_{as}(C=N)	1512 s	1484	1478	1474	1487
ν_s(C=N)	1457, 1393 m	1410	1422, 1368	1414	1418
δ ring	1273 s	1307	1273	1264	1307
δ $(CNNC)_{ip}$	1128, 1098 w	1128, 1110	1110	1128	1106
ν(N—N)	1085, 1055 m	1042	1081	1046	1046
δ_{as} $(C—SH)_{ip}$	948 w	948 vw	948 vw	948 vw	948 vw
δ_s $(C—SH)_{ip}$	923 w	923 vw	923 vw	923 vw	923 vw
ν_{as}(C—S)	756,722 s	743	730	730	743
ν_s(C—S)	662 vw	683	670	–	675
ν_{as}(C—S′)	585 w	589	572	580	589
ν_s(C—S′)	542 vw	551	546	542	551
νH_2O	–	–	3368	3431 w	–
Bend. H_2O			1632	1620 w	

v, very; w, weak; ν, stretch; δ, deformation; s, symmetric; as, antisymmetric; ip, in-plane; bend, bending.

ucts. The noticeable shift in position of the ν_{as}(C=N), ν_s(C=N) and δ ring for the four polymer-metal complexes compared to DMT, is assurance of formation the products.

The starting material DMT showed many bands and broadband absorptions in the range 3100–1800 cm^{-1}. All these bands are attributed to overtones and combinations, except two bands that appeared at 2519 and 2485 cm^{-1} corresponding to the ν_{as}(S—H) and ν_s(S—H), respectively. The broadening of these features might be due to the presence of extensive hydrogen bonding of SH groups.[15]

The adsorbed water absorption bands appeared at 3000–3500 cm^{-1} of ν(H_2O) and bending (H_2O) around (1630 cm^{-1}). They reflect the amount of adsorbed water in each metal complex. For example, the Ni complex, which has six molecules of water, showed a clear band at 3389 cm^{-1}, whereas the Zn complex with no adsorbed water did not show such a band.[16]

The electronic spectra

The main UV-visible absorptions of poly[di(2,5-dimercapto-1,3,4-thiadiazole)-metal] complexes are summarized in Table III.

All the materials showed two or three π–π* (K-band) λ_{max} at 200–270 nm and another two *n*–π* (R-band) at λ_{max} 335–465 nm characterized as ligand-to-metal charge transfer.[17] The charge transfer transition band showed up in the visible region for each of the four polymer-metal complexes namely, PDMT-Co, PDMT-Ni, PDMT-Cu, and PDMT-Zn at 465, 445, 420, and 465 nm, respectively. This proves the metal complexation and that the bands are due to L→M.[18,19]

TABLE III
Main UV-Visible Absorptions of Poly[di(2,5-dimercapto-1,3,4-thiadiazole)-metal] Complexes

Polymer-metal complexes	π-π*			n-π*		
	ν_{max} nm	ν_{max} (cm^{-1})	E_a (eV)	ν_{max} nm	ν_{max} (cm^{-1})	E_a (eV)
DMT	220	45,500	5.6	355	28,200	3.5
	230	43,500	5.4			
	270	37,040	4.6			
PDMT-Co	200	50,000	6.2	355	28,200	3.5
	240	41,700	5.2	465	21,500	2.7
	270	37,040	4.6			
PDMT-Ni	240	41,700	5.2	350	28,600	3.5
	270	37,040	4.6	445	22,500	2.8
PDMT-Cu	200	50,000	6.2	360	27,800	3.4
	230	43,500	5.4	420	23,800	3.0
	270	37,040	4.6			
PDMT-Zn	200	50,000	6.2	335	28,200	3.5
	220	45,500	5.6	465	21,500	2.7
	270	37,040	4.6			

TABLE IV
Thermal Gravimetric Data of Poly[di(2,5-dimercapto-1,3,4-thiadiazole-metal] Complexes

Polymer-metal complexes	Step	TGA Wt. loss % found (Calc.)	T_i/°C	T_f/°C	T_{DrTGA}	Res. % f(Calc.)	E_a kJ mol^{-1} (E_a eV)	React
PDMT-Co	1st	34.880 (34.69)	242	330	297	65.12 (65.31)	227.7 (2.36)	41.5% bb
	2nd	17.076 (16.23)	330	413	359	48.037 (49.08)	338.7 (3.51)	19.4% bb
	3rd	17.850 (16.23)	413	490	454	30.037 (32.85)	351.2 (3.64)	19.4% bb
PDMT-Ni	1st	7.532 (7.74)	25	175	66	92.468 (92.26)	149.6 (1.55)	$-2H_2O$
	2nd	35.680 (35.03)	175	438	352	56.788 (75.23)	62.7 (0.65)	$-4H_2O$ + 22.4% bb
	3rd	13.337 (12.74)	438	795	741	43.451 (44.76)	310.7 (3.22)	14.3% bb
PDMT-Cu	1st	40.553 (40.20)	187	350	309	59.447 (59.80)	84.9 (0.88)	$2H_2O$ + 25.7% bb
	2nd	15.375 (14.570)	620	717	687	44.072 (45.23)	375.3 (3.89)	16.3 % bb
PDMT-Zn	1st	33.764 (33.948)	244	356	319	64.985 (66.05)	224.8 (2.33)	41.5% bb
	2nd	31.14 (31.76)	427	504	470	33.85 (34.261)	217.1 (2.25)	38.9% bb

bb, backbone.

The thermal analysis

Compositional changes as a function of temperature were studied via thermal analysis (TGA and DTA). The difference in the thermal decomposition behavior of the four poly[di(2,5-dimercapto-1,3,4-thiadiazole)]-metal complexes under a nitrogen atmosphere can be seen clearly in their TGA curves. For each step in the decomposition sequence, it was possible to determine the following thermal parameters; T_i, T_f, T_{DTG}, Δm, and E_a which are summarized in Table IV.

The TGA curve (Fig. 1) of the PDMT-Ni indicates that this complex loses its two adsorbed water molecules (Found 65.31%, Cal 65.12%) at the first-step (25–175°C) with a T_{DTG} of 66°C, while the TGA curves of the other complexes indicate the absence of adsorbed water and they are thermally stable in the 25–225°C range. The 25–225°C range is a range of interest at which the DC electrical conductivity measurements were carried out. The water content of the complexes was confirmed by thermal and elemental analyses: six for Ni and two for Cu.

The range 175°C $\leq T \leq$ 900°C is assigned for the release of coordinated water[20] and material decomposition taking place either in two or three steps. Complete details of decomposition and the associated activation energies are summarized in Table IV.

X-ray diffraction patterns

The most direct method of investigation of the structure of the polymer (crystalline and amorphous) is the X-ray diffraction analyses (XRD).[21] All the X-ray diffractographs indicated crystalline structures for the three polymer-metal complexes (PDMT-Co, PDMT-Cu, and PDMT-Zn) while the PDMT-Ni showed an amorphous structure.

From the XRD patterns observed the degree of crystallinity was based on the total intensity of the diffraction peaks of these polymer-metal complexes.[22] They follow the order PDMT-Cu > PDMT-Co > PDMT-Zn >>> PDMT-Ni. Why is the PDMT-Ni amorphous? Because the PDMT-Ni has six molecules of water, two as absorbed water and four as coordinated water. The PDMT-Cu has two molecules

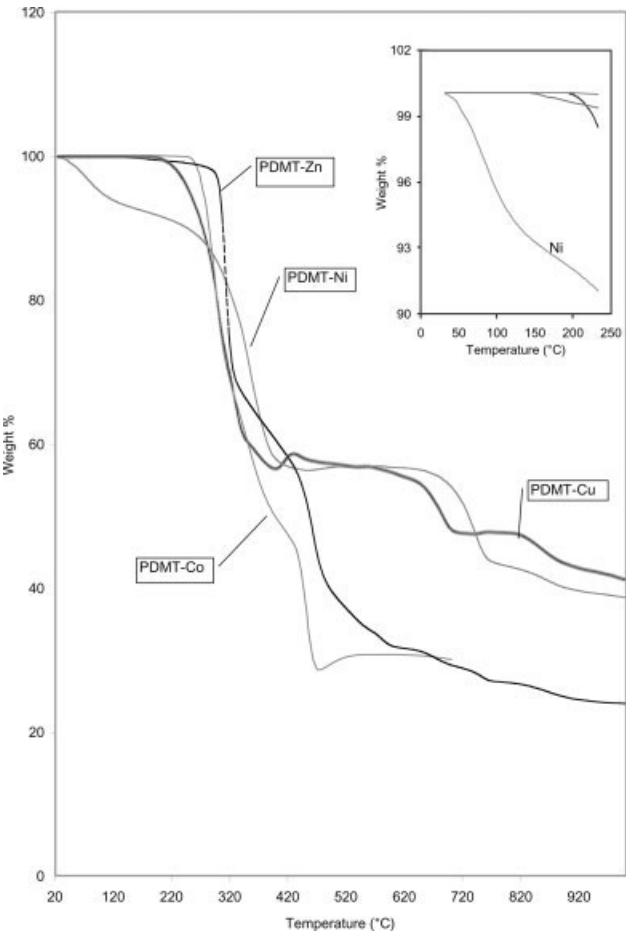

Figure 1 TGA curves of the poly[di(2,5-dimercapto-1,3,4-thiadiazole)]-metal complexes. The insert is the temperature range studied in the DC electrical conductivity.

TABLE V
DC Electrical Conductivity of the Annealed and Doped Poly[di(2,5-dimercapto-1,3,4-thiadiazole)-metal] Complexes

Polymer-metal complex	Annealed (100°C/24 h) S cm^{-1}		Doped (5% I_2) S cm^{-1}	
	300 K	500 K	300 K	500 K
PDMT-Co	1.0×10^{-13}	2.8×10^{-10}	1.2×10^{-13}	1.0×10^{-9}
PDMT-Ni	2.0×10^{-13}	1.6×10^{-8}	1.0×10^{-13}	7.6×10^{-9}
PDMT-Cu	1.0×10^{-10}	1.2×10^{-6}	2.4×10^{-10}	9.0×10^{-7}
PDMT-Zn	1.0×10^{-12}	2.6×10^{-8}	2.6×10^{-11}	3.2×10^{-8}

as coordinated water while PDMT-Co and PDMT-Zn does not have any water. This is confirmed by CHNS elemental analyses, TGA, and FTIR.

DC electrical conductivity

The DC electrical conductivity of the polymer-metal complexes was measured versus $1000/T$ in the range 300–500 K. The effect of the annealing and the acceptor doping with 5% I_2 of the four polymer-metal complexes after annealing upon conductivity is measured and compared. The DC electrical conductivity of the annealed and doped poly[di(2,5-dimercapto-1,3,4-thiadiazole)-metal] complexes are summarized in Table V. All the polymer-metal complexes responded to heat by an increase in the electrical conductivity and behaved almost similarly; this is a typical behavior of semiconductor materials.[23,24] All annealed and doped polymer-metal complexes showed two stages or steps that mean, each one has two activation energies, except PDMT-Co which displayed five stages. Most of these breaks maybe attributed to phase transition; this is confirmed by the small peak in the same range in the DTA that does not correspond to weight loss in the TGA curve.

Figure 2 shows the behavior of the electrical conductivity versus $1000/T$ in the range 300–500 K for the annealed polymer-metal complexes. All the polymer-metal complexes started the DC electrical conductivity at ambient temperature at 10^{-13} S cm^{-1} except PDMT-Cu, which started at 10^{-10} S cm^{-1}. They all showed an increase in the DC electrical conductivity by heat. The DC electrical conductivity of the polymer-copper complex is known to be outstandingly high as noted in these laboratories.[16,19,25] The DC electrical conductivity of the annealed PDMT-Cu is higher than the other materials by three or four orders of magnitude at ambient and higher temperatures. The lowest DC electrical conductivity was for the annealed PDMT-Co at ambient and high temperatures.

The DC electrical conductivity versus $1000/T$ of the 5% I_2 doped poly[di(2,5-dimercapto-1,3,4-thiadiazole)]-metal complexes are displayed in Figure 3. The highest DC electrical conductivity at ambient and higher temperature was noticed for the doped PDMT-Cu, while the lowest DC electrical conductivity is noticed for the doped PDMT-Ni at ambient temperature. The second highest DC electrical conductivity at ambient and higher temperature was observed for the doped PDMT-Zn. In addition, the same trend in this case (doping) together with the annealed case, all the polymer-metal complexes showed two stages (two activation energies) except PDMT-Co, which displayed five stages.

Figure 4 shows the DC electrical conductivity versus $1000/T$ of the annealed and doped (5% I_2) poly [di(2,5-dimercapto-1,3,4-thiadiazole)]-Co(II) complex.

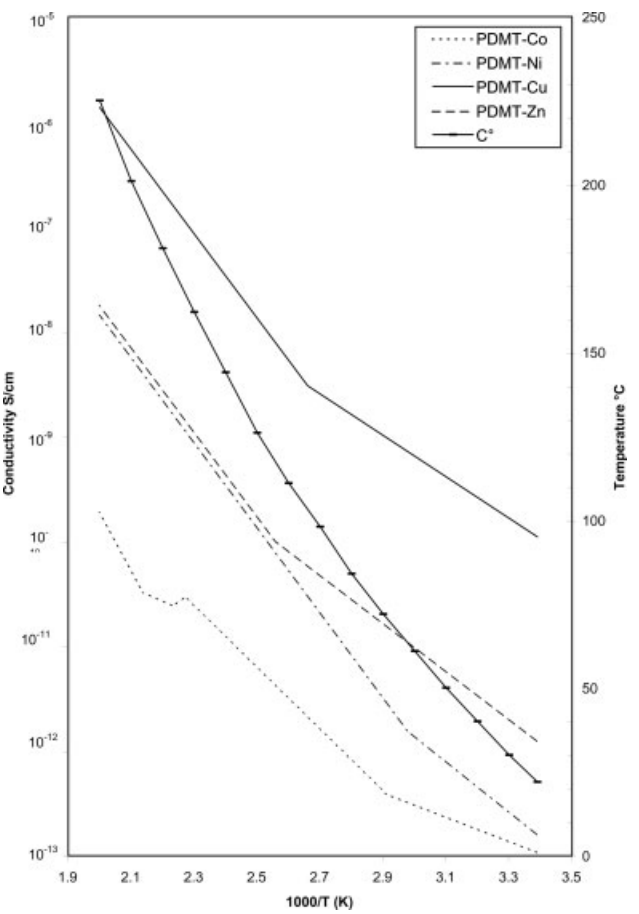

Figure 2 DC electrical conductivity versus $1000/T$ of the annealed poly[di(2,5-dimercapto-1,3,4-thiadiazole)]-metal complexes.

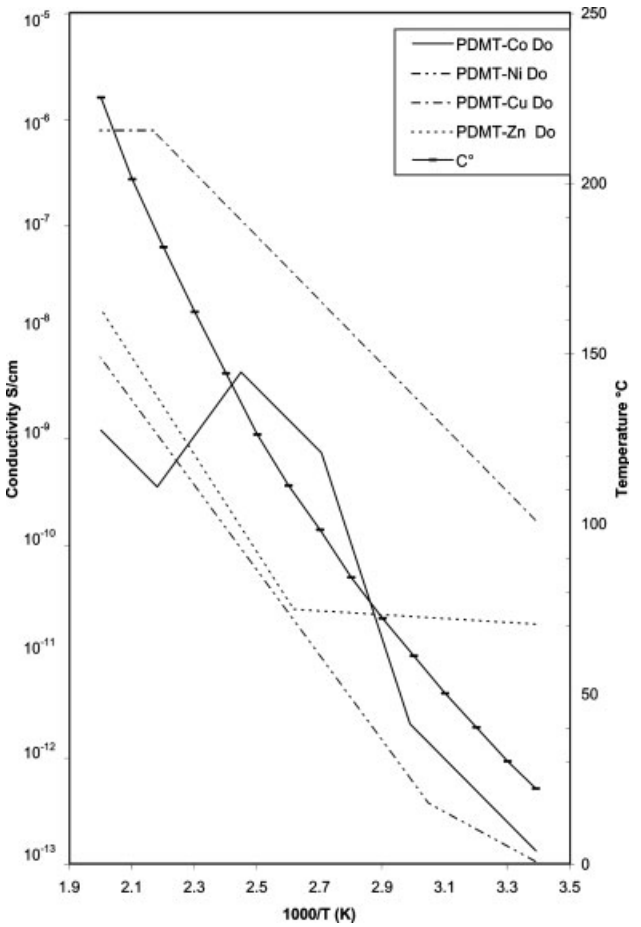

Figure 3 DC electrical conductivity versus $1000/T$ of the doped (5% I2) poly[di(2,5-dimercapto-1,3,4-thiadiazole)]-metal complexes.

The highest DC electrical conductivity at ambient and higher temperature is noticed for the doped PDMT-Co. Also, the enhancement of DC electrical conductivity started at ambient temperature from 10^{-13} S cm^{-1} in the two cases. The doped PDMT-Co gave a DC electrical conductivity of 1.0×10^{-9} S cm^{-1} at high temperature, while the annealed PDMT-Co gave the DC electrical conductivity of 1.4×10^{-10} S cm^{-1}.

There are five slopes for each state. The slopes can be divided into two kinds:

1. Those which have an increase in the DC electrical conductivity (25–71°C), (71–167°C), and (193–225°C) of the annealed state; for the doped state (25–61°C), (61–98°C), (98–136°C), and (185–225°C).
2. Those which have a decrease in DC electrical conductivity of the annealed state (167–173°C) and of the doped state (136–185°C).

All these breaks maybe attributed to phase transition. These are in accordance with the small peaks near these ranges as a T_i in the DTA, which does not correspond to weight loss in the TGA.

Figure 5 shows the DC electrical conductivity versus $1000/T$ of the annealed and 5% I_2 doped poly [di(2,5-dimercapto-1,3,4-thiadiazole)]-Ni(II) complex. The insertion in Figure 5 illustrates the loss of adsorbed water in the TGA. The highest DC electrical conductivity at ambient and higher temperature is noticed for the annealed PDMT-Ni. This is not in accordance with the normal case. Usually the doped materials give higher conductivities, however, these materials have metals in their backbone and the salts of these metals are known to be good dopants, like $ZnCl_2$. Thus these materials are doped internally,[26] and the external doping will not enhance the DC electrically conductivity that much. In the PDMT-Ni, six molecules of water, two adsorbed and four coordinated, were confirmed by elemental analyses, FTIR and TGA. The XRD patterns showed an amorphous structure. This explains why the PDMT-Ni gave the lowest DC electrical conductivity, since the crystallinity is one of the important factors that affect the DC electrical conductivity. The decrease of DC elec-

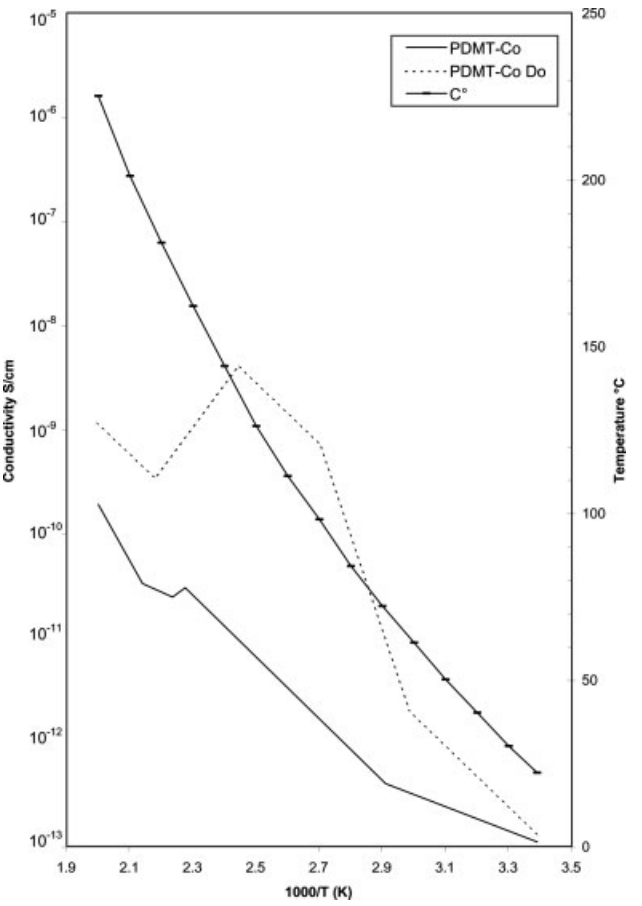

Figure 4 DC electrical conductivity versus $1000/T$ of the annealed and doped (5% I_2) poly[di(2,5-dimercapto-1,3,4-thiadiazole)]-Co(II) complex.

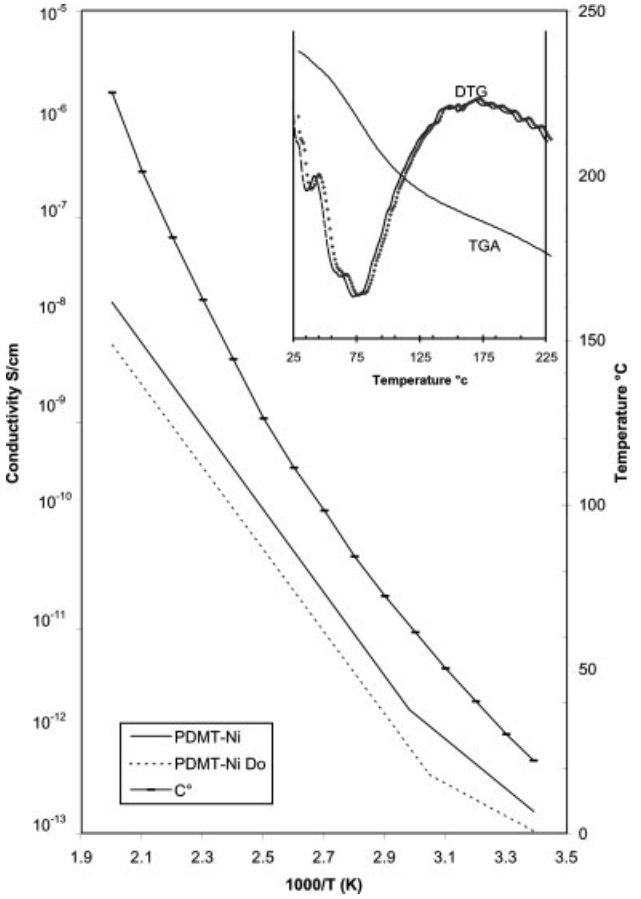

Figure 5 DC electrical conductivity versus $1000/T$ of the annealed and doped (5% I_2) poly[di(2,5-dimercapto-1,3,4-thiadiazole)]-Ni(II) complex.

trical conductivity of the doped PDMT-Ni compared to the annealed PDMT-Ni maybe attributed to the doping with acceptor I_2 that causes a decrease in crystallinity[27] in this configuration. There were two steps for each state: the end of the first step was 66°C. This is confirmed by the appearance of an endothermic peak in the DTA and the maximum temperature to lose the adsorbed water by the TGA (DTG) was near (66 ± 4)°C. The second step was from (66 ± 4)°C to 225°C. The annealed and doped PDMT-Ni gave the DC electrical conductivity of 2.0×10^{-13} and 1.0×10^{-13} S cm^{-1} at ambient temperature and 1.0×10^{-8} and 7.6×10^{-9} S cm^{-1} at 225°C, respectively.

Figure 6 shows the DC electrical conductivity versus $1000/T$ of the annealed and doped poly[di(2,5-dimercapto-1,3,4-thiadiazole)]-Cu(II) complex. The highest DC electrical conductivity at ambient and higher temperature is noticed for doped PDMT-Cu and the enhancement started at ambient temperature for the annealed and doped states. The annealed and doped PDMT-Cu gave a DC electrical conductivity of 1.0×10^{-10} and 2.4×10^{-10} S cm^{-1} at ambient temperature and 2.4×10^{-6} and 9.0×10^{-7} S cm^{-1} at 500 K, respectively. The breaks at 101°C and 185°C in the DC electrical conductivity curve maybe attributed to phase change. This is confirmed by the appearance of endothermic peaks at about the same range in the DTA, which does not show a weight loss in the TGA curve.

Figure 7 shows the DC electrical conductivity versus $1000/T$ of the annealed and doped poly[di(2,5-dimercapto-1,3,4-thiadiazole)]-Zn(II) complex. The highest DC electrical conductivity at ambient and higher temperature was noticed for doped PDMT-Zn and the increase started at ambient temperature for annealed state, while the doped state start the enhancement at 112°C. The annealed and doped PDMT-Zn gave a DC electrical conductivity of 1.0×10^{-12} and 2.6×10^{-11} S cm^{-1} at ambient temperature and 2.6×10^{-8} and 3.2×10^{-8} S cm^{-1} at 225°C, respectively. The breaks at (112 ± 4)°C in the DC electrical curve for both states, maybe assigned to phase transition, which does not correspond to weight loss in the TGA curve, whereas the (112 ± 4)°C in the DTA curve was between endothermic and exothermic peaks.

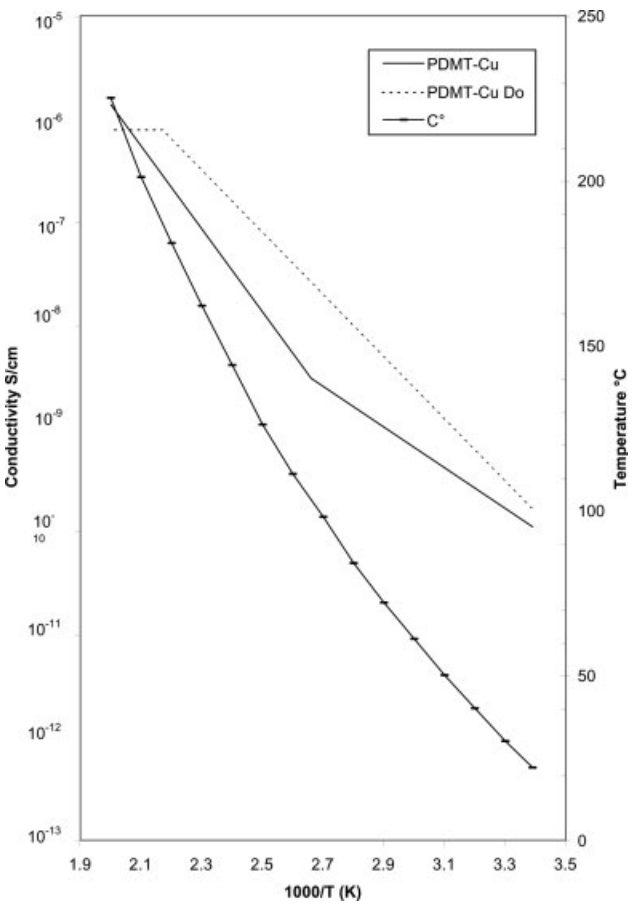

Figure 6 DC electrical conductivity versus $1000/T$ of the annealed and doped (5% I_2) poly[di(2,5-dimercapto-1,3,4-thiadiazole)]-Cu(II) complex.

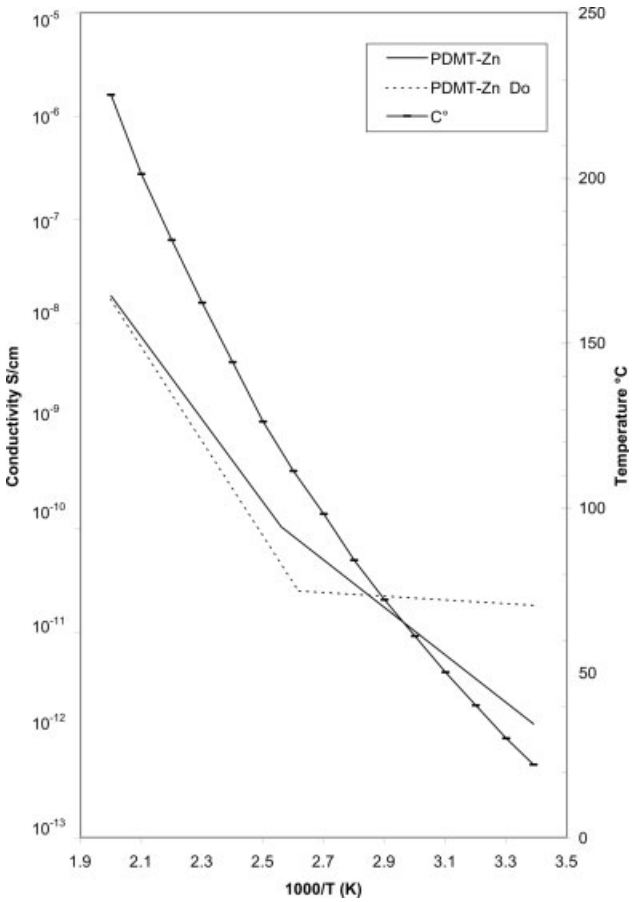

Figure 7 DC electrical conductivity versus $1000/T$ of the annealed and doped poly[di(2,5-dimercapto-1,3,4-thiadiazole)]-Zn(II) complexes.

Activation energies

The carriers available for the DC electrical conductivity are electrons and holes. The calculations for the bulk activation energies (E_a) at different temperature ranges for all the segments of the curves of the annealed and doped polymer complexes are summarized in Table VI.

The PDMT-Co gave five activation energies, while the remaining three polymer-metal complexes (Ni, Cu, and Zn) showed two segments and two activation energies each. All these segments are due to physical reactions (phase transitions or chain conformation) as confirmed by DTA. The segment of PDMT-Ni is an exception. It is due to the release of the two molecules of adsorbed water.[16] This is also confirmed later by TGA.

To explain the Figures 2–6 of DC electrical conductivity versus $1/T$ of the annealed and doped PDMT-M's, let us introduce Figure 8, which presents an energy schematic model based on the band theory. In our case, the bulk energy gap (BEG) is about 1.6 eV. This is the highest activation energy obtained.

There is many data to explain the activation energies for the four polymer-metal complexes in the annealed and doped states. The annealed and doped PDMT-Cu is taken as an example.

For the annealed PDMT-Cu, the first segment is due to the excitation from the upper levels of the negative bipolarons (BP^-), which is $\sim$ 0.4 eV below the bulk conduction band (BCB). The second segment is due to a soliton (S^-) level excitation [i.e. in the middle of bulk energy gap (BEG)[28]] which is a bout 0.8 eV.

In the doped state, the first segment is due to the excitation from the upper level of negative polaron (P^-), which is $\sim$ 0.6 eV. The second segment (0.0 eV) is due to recombination and annihilation (R).

From this, there is a close correspondence between the DC electrical conductivity, the energy diagram schematic model based on the band theory, TGA, DTA, CHNS analysis, and X-ray diffraction. This is clearly illustrated in case of especially PDMT-Ni.

TABLE VI
Calculations for the Bulk Activation Energies (E_a) at Different Temperature Ranges of Annealed and Doped Polymer-Metal Complexes

	Annealed (100°C/24 h)			Doped (5% I_2)		
Polymer-metal complex	T (°C)	E_a eV		T (°C)	E_a eV	
PDMT-Co	25–71	0.4	BP^-	22–62	0.6	P^-
	71–166	0.6	P^-	62–97	1.6	VB
	166–174	+eV	–	97–135	0.6	P^-
	174–194	0.4	R	153–185	+eV	–
	194–225	1.2	BP^-	185–225	0.6	P^-
PDMT-Ni	25–63	0.5	W	25–56	0.6	W
	63–225	0.8	S	56–225	0.8	S
PDMT-Cu	25–103	0.4	BP^-	25–187	0.6	P^-
	103–225	0.8	S	187–225	0.0	R
PDMT-Zn	25–115	0.4	BP^-	25–108	0.0	R
	115–225	0.8	S	108–225	0.8	S

R, recombination and annihilation; VB, valence band; W, water release; S, soliton; BP, bipolaron.

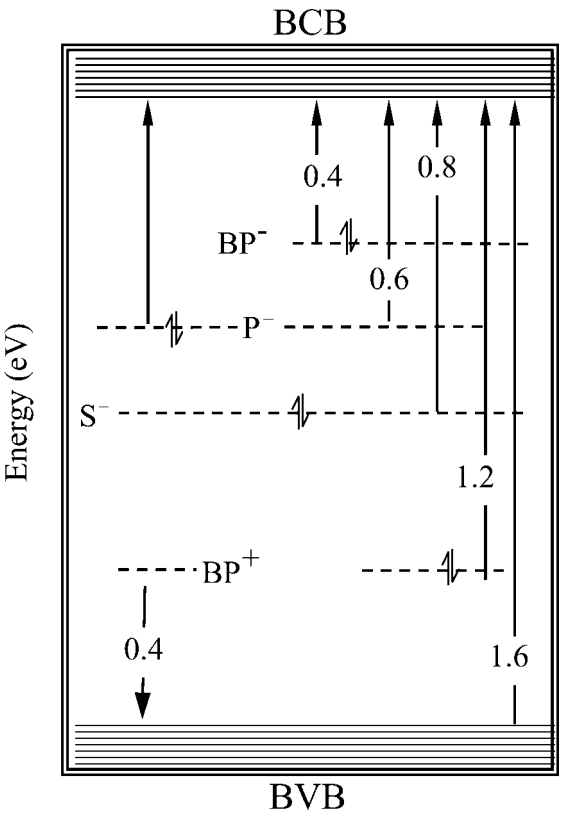

Figure 8 Proposed energy schematic model based on the band theory of the polymer-metal complexes.

CONCLUSIONS

The following points can be concluded from this work:

1. Reaction of the 2,5-dimercapto-1,3,4-thiadiazole with anhydrous metal chlorides formed polymer-metal complexes of the type $[ML_2]_n$. Their chemical and physical properties are studied.
2. The correlations between CHNS analysis, TGA, DTA, X-ray diffraction, and DC electrical conductivity for the polymer-metal complexes are followed.
3. From the X-ray diffraction, the crystallinity follow the order PDMT-Cu > PDMT-Co > PDMT-Zn >>> PDMT-Ni. The amorphous structure of the PDMT-Ni is attributed to presence two molecules of adsorbed water.
4. All the polymer-metal complexes are thermally stable at 300–500 K, except PDMT-Ni because of release the adsorbed water.
5. The electrical conductivity of all polymer complexes, whether annealed or doped, increased with increasing temperature. This is mainly due to the variation of the carrier concentration with temperature as in the case of semiconductors.
6. The polymer-metal complexes have metals in their backbones and the salts of these metals are known to be good dopants. Thus, these materials are doped internally, so the doped polymer-metal complexes are only one or two orders of magnitude higher in DC electrical conductivity than the annealed state.

References

1. El-Shekeil, A.; Babaqi, A.; Hassan, M. A.; Sheba, S. Heterocycles 1988, 27, 2577.
2. El-Shekeil, A.; Babaqi, A.; Hassan, M. A.; Sheba, S. Acta Chim Hung 1989, 126, 813.
3. Kucharski, A.; Mieczyslaw, J. Appl Polym Sci 2000, 76, 439.
4. Jinxia, L.; Zhan, H.; Zhou, Y. Electrochem Commun 2003, 5, 555.
5. Nalwa, H. S., Ed. Handbook of Organic Conductive Molecules and Polymers, Vol. 2; Wiley: New York, 1997.
6. Kiess, H. G., Ed. Conjugated Conducting Polymers, Springer Series in Solid State Science; Springler: Berlin, 1992; p 102.
7. Mort, J.; Pfister, G., Ed. Electronic Properties of Polymers; Wiley: New York, 1982.
8. Marvel, C. S.; Torkoy, N. J Am Chem Soc 1957, 79, 6000.
9. Katon, J., Ed. Organic Semiconducting Polymers; Marcel Dekker: New York, 1968.
10. Singh, N.; Kumar, R. Inorg Chem Commun 2003, 6, 97.
11. El-Shekeil, A.; Khalid, M.; Al-Yusufy, F. Macromol Chem Phys 2001, 202, 2971.
12. Coats, A. W.; Redfern, J. P. Nature 1964, 68, 201.
13. Horovitz, H. H.; Metzger, G. Anal Chem 1963, 35, 1464.
14. Edwards, H. G. M.; Johnson, A. F.; Lawson, E. E. J Mol Struct 1995, 351, 51.
15. Bellamy, L. J. The Infrared Spectra of Complex Molecules, Vol. 1; Wiley: New York, 1975; p 395.
16. El-Shekeil, A.; Khalid, M. A.; Al-Maydama, H.; Al-Karbooly, A. Eur Polym J 2001, 37, 575.
17. El-Shekeil, A.; El-Sonbati, A. Transition Met Chem 1992, 17, 420.
18. Rastogi, D.; Sharma, K. J Inorg Nucl Chem 1967, 36, 2219.
19. Khalid, M. A.; El-Shekeil, A. G.; Al-Yusufy, F. A. Eur Polym J 2001, 37, 1423.
20. Patel, M. N.; Patil, S.; Setty, M. S. Die Agewandte Macromolekulare Chemie 1981, 97, 69.
21. Perepechko, I. I. An Introduction to Polymer Physics; Mir Publishers: Moscow, 1981; p 31.
22. Otsuka, M.; Kato, F.; Matsuda, Y. AAPS PharmSci 2000, 2, article 9.
23. Katon, J. E., Ed. Organic Semiconducting Polymers; Marcel Dekker: New York, 1968; p 40.
24. Nalwa, H. S., Ed. Handbook of Organic Conductive Molecules and Polymers, Vol. 2, Wiley: New York, 1997; p 763.
25. Katon, J. E., Ed. Organic Semiconducting Polymers; Marcel Dekker: New York, 1968; p 61, 100, 115.
26. Nalwa, H. S., Ed. Handbook of Organic Conductive Molecules and Polymers, Vol. 2; Wiley: New York, 1997; p 730.
27. El-Shekeil, A.; Al-Maydamah, H.; Al-Karbooly, A. Polym Adv Technol 1999, 10, 146.
28. Nalwa, H. S., Ed. Handbook of Organic Conductive Molecules and Polymers, Vol. 2; Wiley: New York, 1997; p 16.